

Dynamics of a shallow underground two-layer pipeline under the moving loads

Svetlana Girnis^a , Vitaliy Ukrainets^a , Viktor Stanevich^{a*} , Larisa Gorshkova^a 

^a Faculty of Architecture and Construction, Toraighyrov University, Pavlodar, Kazakhstan. Email: girnis@mail.ru, vitnikukr@mail.ru, svt_18@mail.ru, gorshkova_larisa@mail.ru

* Corresponding author

<https://doi.org/10.1590/1679-78258191>

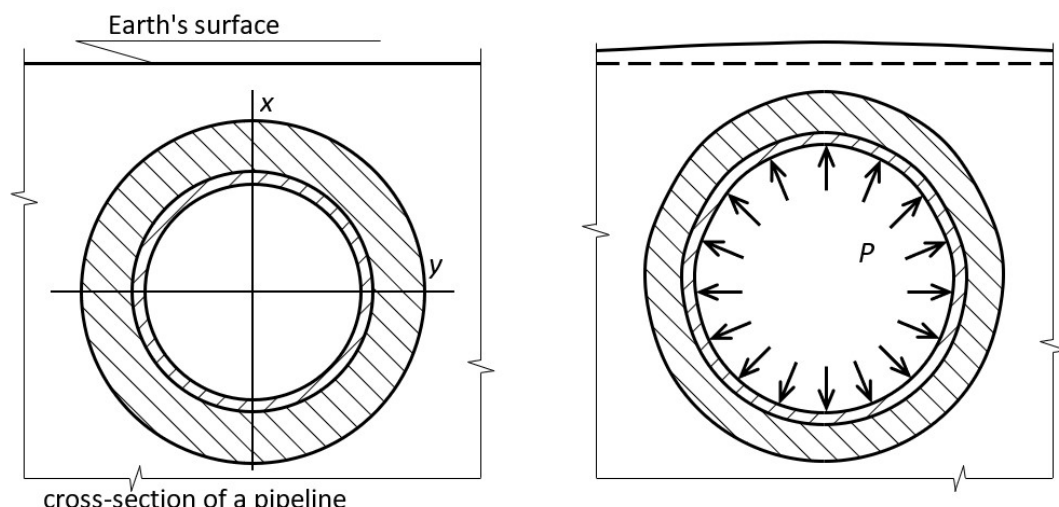
Abstract

The mathematical modeling of the dynamics of a two-layer shallow pipeline under the influence of transport load (the load created by an object moving along the pipeline) has been successfully resolved. The pipeline is represented as an extended circular cylindrical two-layer shell with a thin inner (bearing) layer and a thick outer (enclosing) layer situated in an elastic half-space. Dynamic equations of elasticity theory using Lamé potentials are utilized to describe the motion of the half-space and the enclosing layer of the shell. The vibrations of the bearing layer of the shell are described by the classical equations of the theory of shells. Numerical experiments have considered the case of a moving axisymmetric cylindrical normal load applied to a pipeline (without an enclosing layer and with an enclosing layer of varying thickness and material stiffness). It was demonstrated that if the material of the enclosing layer of the pipeline is more rigid than that of the rock mass, the dynamic effect of the moving load on the rock mass is reduced.

Keywords

Elastic half-space, pipeline, two-layer shell, moving load, displacements, stresses

Graphical Abstract



Received May 10, 2024. In revised form July 29, 2024. Accepted August 29, 2024. Available online September 03, 2024.
<https://doi.org/10.1590/1679-78258191>

 Latin American Journal of Solids and Structures. ISSN 1679-7825. Copyright © 2024. This is an Open Access article distributed under the terms of the [Creative Commons Attribution License](#), which permits unrestricted use, distribution, and reproduction in any medium, provided the original work is properly cited.

1 INTRODUCTION

Currently, underground space is being developed intensively for various purposes. The construction of underground trunk pipelines, which provide transportation of almost the entire volume of produced natural gas, most of the oil, and various cargoes (Kulińska, 2014; Zhangabay et al., 2023), has become extremely widespread. In addition to the static calculation of such structures, their dynamic analysis is necessary (Yerzhanov and Ajtaliev, 1989; Ukrainets, 2006). Among the dynamic loads and impacts on underground pipelines, it is necessary to single out transport loads (loads generated by objects moving through the pipeline) and the impact of seismic waves of natural or artificial origin.

The study of the dynamics of underground pipelines under the influence of transport loads by mathematical modeling approach leads to the emergence of boundary value problems of deformable solid mechanics. As demonstrated by calculations (Ukrainets, 2006) and experimental studies, the impact effect of transport loads on the ground surface diminishes with increasing depth of the pipeline embedment. At a depth of approximately four to five times its characteristic transverse dimensions, such impact effect is negligible. In this case, when addressing the transportation problem, it is possible to disregard the ground surface and consider the pipeline as a deep-buried structure. A bibliography concerning the mathematical modeling of such and similar structures under various loads and impacts can be found in the monographs by Yerzhanov and Ajtaliev (1989), and Ukrainianets (2006).

In a pioneering study, Lvovsky et al. (1974) solved the transportation problem of a deep buried pipeline, whereby a load moves at a constant subsonic velocity on an infinitely long circular cylindrical homogeneous shell in elastic space. However, the application of such a model of an underground pipeline may be limited in the case of its layered structure, consisting of rigidly interconnected concentric layers with different physical and mechanical properties. In this case, the design scheme for a deeply buried pipeline is represented by a similar circular cylindrical layered shell located in elastic space. The dynamics of a free, non-contacting layered shell of considerable length under the influence of a moving load were investigated by Pozhuev (1977, 1978, 1980). Similar studies for a two-layer and three-layer shell in elastic space were conducted by Otarbaev (2016, 2018) and Girnis (2023).

For a shallow pipeline, the solution to the transportation problem becomes considerably more complex due to the perceptible deformation of the ground surface and its influence on stress concentration in the vicinity of the pipeline during the diffraction of reflected waves. In this case, the design scheme for an underground pipeline is represented as an infinitely long circular cylindrical shell located in an elastic half-space. The number of papers devoted to this issue is limited, with the majority of research conducted in recent years. These include Ukrainianets (2006, 2010), Yang and Hung (2008), Alexeyeva (2009, 2020), Hussein et al. (2010, 2014), Coşkun and Dolmaseven (2017), Yuan et al. (2017), Boström and Yuan (2019), Zhou (2019), Makashev (2023), Zhukhova (2023). In these works, similar to (Lvovsky et al., 1974), the action of a moving load on a homogeneous shell is considered. In this paper, the design scheme of a shallow-buried underground pipeline consisting of two concentric layers is represented as an extended circular cylindrical two-layer shell located in an elastic half-space with a thin inner layer and a thick outer layer. It is assumed that the contact between the shell and the surrounding medium, as well as between the shell layers, is rigid.

The objective of this work is to construct an analytical solution to the problem and develop computer programs based on it for studying the dynamics of a shallow-buried underground two-layer pipeline under the influence of transportation load.

2 METHODS

The study employs a mathematical modeling approach, using elasticity theory (Yerzhanov and Ajtaliev, 1989; Ukrainianets, 2006). The underground pipeline is represented as an extended circular cylindrical two-layer shell with a thin inner (bearing) layer and a thick outer (enclosing) layer situated in an elastic half-space parallel to its horizontal boundary. Initially, the load, which moves uniformly with subsonic velocity along the inner surface of the shell, is assumed to be sinusoidal along the shell axis with an arbitrary relation on the angular coordinate. The method of incomplete separation of variables is proposed as a means of solving the problem in this case (Alexeyeva, 2009, 2020; Ukrainianets, 2010; Otarbaev, 2016, 2018; Girnis et al., 2023). The solution for the Lamé potentials is presented as a superposition of Fourier-Bessel series and Fourier-type contour integrals (Ukrainets, 2010; Alexeyeva, 2020). Furthermore, the method of decomposition of potentials into plane waves and decomposition of plane waves into series on cylindrical functions is employed (Alexeyeva, 2009, 2020; Ukrainianets, 2010). It is assumed that the velocity of the load motion should be less than the velocity of Rayleigh waves in the half-space. The obtained solution is then used to solve the problem of the action of a moving load on the given shell, which has no periodicity but is represented as a Fourier integral (Ukrainets, 2010; Alexeyeva, 2020).

3 RESULTS

3.1 Formulation and analytical solution of the problem

Consider a homogeneous, isotropic, and linear-elastic medium (body) bounded by a horizontal plane (half-space) in the cylindrical r, θ, z and Cartesian x, y, z coordinate systems (not changing its position). The boundary of the half-space in the absence of a load is perpendicular to the x -axis, with $x \leq h$. In the half-space, there exists an infinitely long circular cylindrical shell with a two-layer structure. The radius of its outer surface is denoted by R_1 ($R_1 < h$). The axis of the shell is parallel to the boundary of the half-space and coincides with the coordinate z -axis (Fig. 1). The inner (bearing) layer of the two-layer shell is a thin-walled elastic shell with a thickness of h_0 and a radius of the medial surface of R_2 . Given that the shell is thin, it is assumed that it is in contact with the outer (enclosing) layer of the two-layer shell along its medial surface. It is assumed that the contact between the shell and the surrounding body, as well as between the shell layers, is rigid.

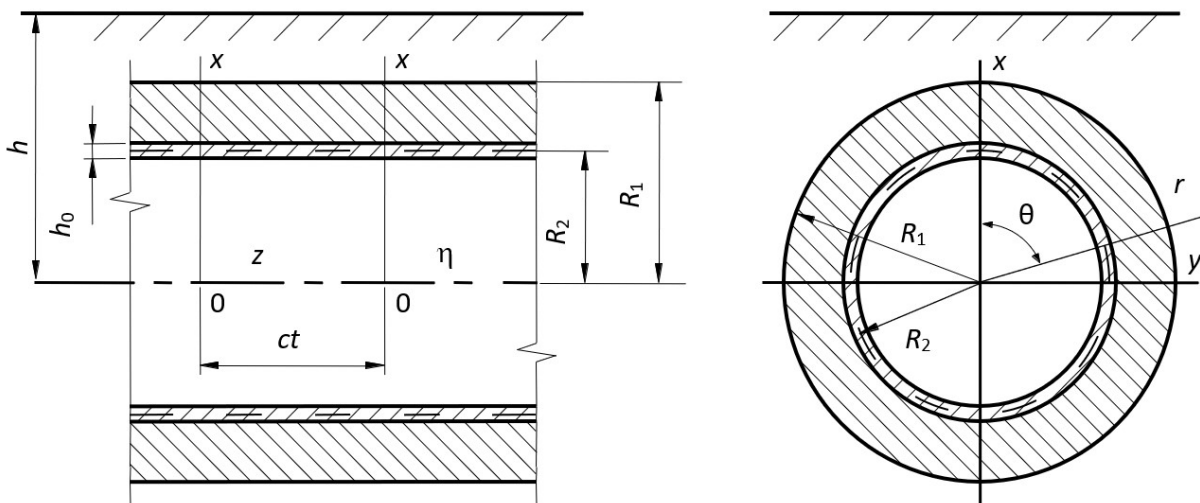


Figure 1 A two-layer shell in an elastic half-space.

The physical and mechanical properties of the materials of the half-space and shell layers are characterized by the following constants: ν_k – Poisson's ratio, μ_k – shear modulus, ρ_k – density ($k = 0, 1, 2$), where index $k = 0$ refers to the load-bearing layer of the shell, $k = 1$ to the half-space, $k = 2$ to the enclosing layer of the shell.

A load of intensity P acts on the inner surface of the shell. The load moves in the direction of the z -axis with a constant velocity c . The velocity of the load is subsonic, i.e., less than the velocities of shear wave propagation in the enclosing layer of the shell and its surrounding body. The stress-strain state (SSS) of the shell and half-space must be determined for this load.

To solve the problem, we must turn to the moving cylindrical ($r, \theta, \eta = z - ct$) and Cartesian ($x, y, \eta = z - ct$) coordinate systems, which must move together with the load (Fig. 1).

The motion of the half-space ($k = 1$) and the enclosing layer of the shell ($k = 2$) will be described by the dynamic equations of elasticity theory in the moving coordinate system (Otarbaev, 2016, 2018; Girnis et al., 2023; Ukrainianets, 2010; Alexeyeva, 2020)

$$\left(M_{pk}^{-2} - M_{sk}^{-2} \right) \text{grad div } \mathbf{u}_k + M_{sk}^{-2} \nabla^2 \mathbf{u}_k = \partial^2 \mathbf{u}_k / \partial \eta^2, \quad k = 1, 2, \quad (1)$$

where $M_{pk} = c/c_{pk}$, $M_{sk} = c/c_{sk}$ – Mach numbers, $c_{pk} = \sqrt{(\lambda_k + 2\mu_k)/\rho_k}$, $c_{sk} = \sqrt{\mu_k/\rho_k}$ – expansion-compression and shear wave propagation velocities, respectively, $\lambda_k = 2\mu_k\nu_k/(1-2\nu_k)$; ∇^2 – Laplace operator, \mathbf{u}_k – point displacement vectors.

In order to describe the motion of the load-bearing layer of the shell, we will employ classical equations derived from the theory of shells in a moving coordinate system (Ukrainets, 2006; Girnis et al., 2023; Alexeyeva, 2009)

$$\begin{aligned} & \left[1 - \frac{(1-\nu_0)\rho_0 c^2}{2\mu_0} \right] \frac{\partial^2 u_{0\eta}}{\partial \eta^2} + \frac{1-\nu_0}{2R^2} \frac{\partial^2 u_{0\theta}}{\partial \theta^2} + \frac{1+\nu_0}{2R} \frac{\partial^2 u_{0\theta}}{\partial \eta \partial \theta} + \frac{\nu_0}{R} \frac{\partial u_{0r}}{\partial \eta} = \frac{1-\nu_0}{2\mu_0 h_0} (P_\eta - q_\eta), \\ & \frac{1+\nu_0}{2R} \frac{\partial^2 u_{0\theta}}{\partial \eta \partial \theta} + \frac{(1-\nu_0)}{2} \left(1 - \frac{\rho_0 c^2}{\mu_0} \right) \frac{\partial^2 u_{0\theta}}{\partial \eta^2} + \frac{1}{R^2} \frac{\partial^2 u_{0\theta}}{\partial \theta^2} + \frac{1}{R^2} \frac{\partial u_{0r}}{\partial \theta} = \frac{1-\nu_0}{2\mu_0 h_0} (P_\theta - q_\theta), \\ & \frac{\nu_0}{R} \frac{\partial u_{0\eta}}{\partial \eta} + \frac{1}{R^2} \frac{\partial u_{0\theta}}{\partial \theta} + \frac{h_0^2}{12} \nabla^2 \nabla^2 u_{0r} + \frac{(1-\nu_0)\rho_0 c^2}{2\mu_0} \frac{\partial^2 u_{0r}}{\partial \eta^2} + \frac{u_{0r}}{R^2} = -\frac{1-\nu_0}{2\mu_0 h_0} (P_r - q_r), \end{aligned} \quad (2)$$

where $R = R_2$; when $r = R$ $q_j = \sigma_{rj2}$, P_j , q_j are the components of the load intensity $P(\theta, \eta)$ and the reaction of the enclosing layer of the shell, u_{0j} , σ_{rj2} are the components of the displacements of the points of the mid-surface of the bearing layer of the shell and the stress tensor in the enclosing layer of the shell, $j = \eta, \theta, r$.

If the vectors \mathbf{u}_k are represented using Lamé potentials ϕ_{jk} ($j = 1, 2, 3$, $k = 1, 2$) (Otarbaev, 2016, 2018; Girnis et al., 2023; Ukrainets, 2010; Alexeyeva, 2020)

$$\mathbf{u}_k = \text{grad } \phi_{1k} + \text{rot} (\phi_{2k} \mathbf{e}_\eta) + \text{rot rot} (\phi_{3k} \mathbf{e}_\eta), \quad k = 1, 2, \quad (3)$$

it follows from (1) and (3) that ϕ_{jk} satisfy the equations

$$\nabla^2 \phi_{jk} = M_{jk}^2 \partial^2 \phi_{jk} / \partial \eta^2, \quad j = 1, 2, 3, \quad k = 1, 2. \quad (4)$$

Here \mathbf{e}_η is the unit vector of the η -axis, $M_{1k} = M_{pk}$, $M_{2k} = M_{3k} = M_{sk}$.

Through the potentials ϕ_{jk} it is possible to express the components of the stress tensors σ_{lmk} in the half-space ($k = 1$) and the enclosing layer of the shell ($k = 2$), related by Hooke's law to the components u_{lk} of the displacement vectors \mathbf{u}_k ($l, m = r, \theta, \eta$, $k = 1, 2$; $l, m = x, y, \eta$, $k = 1$).

$$\begin{aligned} P(\theta, \eta) &= p(\theta) e^{i\xi\eta}, \quad p(\theta) = \sum_{n=-\infty}^{\infty} P_n e^{in\theta}, \\ p_j(\theta, \eta) &= p_j(\theta) e^{i\xi\eta}, \quad p_j(\theta) = \sum_{n=-\infty}^{\infty} P_{nj} e^{in\theta}, \quad j = r, \theta, \eta. \end{aligned} \quad (5)$$

Let us represent the Lamé potentials in the analogous form (5):

$$\phi_{jk}(r, \theta, \eta) = \Phi_{jk}(r, \theta) e^{i\xi\eta}. \quad (6)$$

Substituting (6) into (4), we obtain

$$\nabla_2^2 \Phi_{jk} - m_{jk}^2 \xi^2 \Phi_{jk} = 0, \quad j = 1, 2, 3, \quad k = 1, 2, \quad (7)$$

where ∇_2^2 – two-dimensional Laplace operator, $m_{jk} = \sqrt{1 - M_{jk}^2}$, $m_{1k} = m_{pk}$, $m_{2k} = m_{3k} = m_{sk}$.

The application of (6) allows for the derivation of expressions for displacements u_{lk}^* and stresses σ_{lmk}^* ($l, m = r, \theta, \eta$) within the half-space ($k = 1$) and the enclosing layer of the shell ($k = 2$), as well as u_{lm1}^* , σ_{lm1}^* ($l, m = x, y, \eta$) within the half-space, in response to a sinusoidal load (5) as a function of Φ_{jk} (* means that these components correspond to the case of a sinusoidal moving load (5) acting on the shell).

Given that $c < c_{sk}$ ($k = 1, 2$), $M_{sk} < 1$, and the solutions to equations (7) can be represented as (Ukrainets, 2010; Alexeyeva, 2020)

$$\Phi_{jk} = \Phi_{jk}^{(1)} + \Phi_{jk}^{(2)}, \quad j=1,2,3, \quad k=1,2, \quad (8)$$

where:

- for half-space

$$\Phi_{j1}^{(1)} = \sum_{n=-\infty}^{\infty} a_{nj} K_n(k_{j1}r) e^{in\theta}, \quad \Phi_{j1}^{(2)} = \int_{-\infty}^{\infty} g_j(\xi, \zeta) \exp\left(iy\zeta + (x-h)\sqrt{\zeta^2 + k_{j1}^2}\right) d\zeta;$$

- for enclosing layer of the shell

$$\Phi_{j2}^{(1)} = \sum_{n=-\infty}^{\infty} a_{nj+3} K_n(k_{j2}r) e^{in\theta}, \quad \Phi_{j2}^{(2)} = \sum_{n=-\infty}^{\infty} a_{nj+6} I_n(k_{j2}r) e^{in\theta}.$$

Here $I_n(k_j r)$, $K_n(k_j r)$ are the modified Bessel functions and McDonald functions, $k_{j1} = |m_{j1}\xi|$, $k_{j2} = |m_{j2}\xi|$; a_{n1}, \dots, a_{n9} , $g_j(\xi, \zeta)$ are the unknown coefficients and functions, $j = 1, 2, 3$.

In the Cartesian coordinate system, the expressions for the potentials Φ_{j1} (8) will take the form (Ukrainets, 2010; Alexeyeva, 2020)

$$\Phi_{j1} = \int_{-\infty}^{\infty} \left[\frac{e^{-xf_j}}{2f_j} \sum_{n=-\infty}^{\infty} a_{nj} \Phi_{nj} + g_j(\xi, \zeta) e^{(x-h)f_j} \right] e^{iy\zeta} d\zeta, \quad (9)$$

where $f_j = \sqrt{\zeta^2 + k_{j1}^2}$, $\Phi_{nj} = [\zeta + f_j]/k_{j1}$, $j = 1, 2, 3$.

The functions $g_j(\xi, \zeta)$ will be expressed through the coefficients a_{nj} ($j = 1, 2, 3$). In order to achieve this, it is necessary to consider the boundary conditions on the boundary of the half-space $x = h$, as set out in equation (9):

$$\sigma_{xx1}^* = \sigma_{xy1}^* = \sigma_{x\eta1}^* = 0.$$

By equating the coefficients when $e^{iy\zeta}$ to zero, we obtain a system of three algebraic equations. From this system of equations we will find

$$g_j(\xi, \zeta) = \frac{1}{\Delta_*} \sum_{l=1}^3 \Delta_{jl}^* e^{-hf_l} \sum_{n=-\infty}^{\infty} a_{nl} \Phi_{nl}. \quad (10)$$

Here $\Delta_* = (2\rho_*^2 - \beta^2)^2 - 4\rho_*^2 \sqrt{\rho_*^2 - \alpha^2} \sqrt{\rho_*^2 - \beta^2}$,

$$\Delta_{11}^* = \frac{\Delta_*}{2\sqrt{\rho_*^2 - \alpha^2}} - \frac{(2\rho_*^2 - \beta^2)^2}{\sqrt{\rho_*^2 - \alpha^2}}, \quad \Delta_{12}^* = -2\xi(2\rho_*^2 - \beta^2), \quad \Delta_{13}^* = 2\xi(2\rho_*^2 - \beta^2) \sqrt{\rho_*^2 - \beta^2},$$

$$\Delta_{21}^* = -\frac{M_{s1}^2}{m_{s1}^2} \Delta_{11}^*, \quad \Delta_{22}^* = -\frac{\Delta_{**}}{2\sqrt{\rho_*^2 - \beta^2}}, \quad \Delta_{23}^* = -4\xi\zeta \frac{M_{s1}^2}{m_{s1}^2} \sqrt{\rho_*^2 - \alpha^2} \sqrt{\rho_*^2 - \beta^2},$$

$$\Delta_{31}^* = -\frac{\Delta_{13}^*}{m_{s1}^2 \xi^2}, \quad \Delta_{32}^* = \frac{\Delta_{21}^*}{\beta^2}, \quad \Delta_{33}^* = -\frac{\Delta_{**}}{2\sqrt{\rho_*^2 - \beta^2}} + \frac{(2\rho_*^2 - \beta^2)^2}{\sqrt{\rho_*^2 - \beta^2}},$$

$$\alpha = M_{pl}\xi, \quad \beta = M_{sl}\xi, \quad \rho_*^2 = \xi^2 + \zeta^2, \quad \Delta** = \left(2\rho_*^2 - \beta^2\right)^2 - 4\rho_*^2\sqrt{\rho_*^2 - \alpha^2}\sqrt{\rho_*^2 - \beta^2},$$

$$\rho_*^2 = \xi^2 + \left(2/m_{sl}^2 - 1\right)\zeta^2.$$

In Ukrainianets (2006) it is proved that the determinant $\Delta*(\xi, \zeta)$ does not turn into zero at any ζ values when $c < c_R$, where c_R is the velocity of Rayleigh surface waves in a half-space (Novackij, 1975). It is important to note that in real media c_R is slightly less than the shear wave velocity.

When $c < c_R$ the expressions for the potentials Φ_{j1} in the Cartesian coordinate system (9), taking into account (10), are as follows

$$\Phi_{j1} = \int_{-\infty}^{\infty} \left[\frac{e^{-xf_j}}{2f_j} \sum_{n=-\infty}^{\infty} a_{nj} \Phi_{nj} + e^{(x-h)f_j} \sum_{l=1}^3 \frac{\Delta_{jl}^*}{\Delta_*} e^{-hf_l} \sum_{n=-\infty}^{\infty} a_{nl} \Phi_{nl} \right] e^{iy\zeta} d\zeta.$$

In the cylindrical coordinate system when $c < c_R$ the expressions for the potentials Φ_{j1} (8) taking into account (10) and using the relation (Yerzhanov and Ajtaliev, 1989)

$$\exp\left(iy\zeta + (x-h)\sqrt{\zeta^2 + k_j^2}\right) = \sum_{n=-\infty}^{\infty} I_n(k_j r) e^{in\theta} \left[\left(\zeta + \sqrt{\zeta^2 + k_j^2} \right) / k_j \right]^n e^{-h\sqrt{\zeta^2 + k_j^2}},$$

become as follows

$$\Phi_{j1} = \sum_{n=-\infty}^{\infty} \left(a_{nj} K_n(k_j r) + b_{nj} I_n(k_j r) \right) e^{in\theta}.$$

$$\text{Here } b_{nj} = \sum_{l=1}^3 \sum_{m=-\infty}^{\infty} a_{ml} A_{nj}^{ml}, \quad A_{nj}^{ml} = \int_{-\infty}^{\infty} \frac{\Delta_{jl}^*}{\Delta_*} \Phi_{ml} \Phi_{nj} e^{-h(f_l + f_j)} d\zeta.$$

Let us substitute the relations found in the cylindrical coordinate system for the potentials Φ_{jk} into the expressions for displacements u_{lk}^* and stresses σ_{lmk}^* ($l, m = r, \theta, \eta$) in the half-space ($k = 1$) and in the enclosing layer of the shell ($k = 2$). Then only the coefficients a_{n1}, \dots, a_{n9} are unknown in these expressions:

$$u_{l1}^* = \sum_{n=-\infty}^{\infty} \sum_{j=1}^3 \left[T_{lj1}^{(1)} \left(K_n(k_j r) \right) a_{nj} + T_{lj1}^{(2)} \left(I_n(k_j r) \right) b_{nj} \right] e^{i(\xi\eta + n\theta)},$$

$$\frac{\sigma_{lm1}^*}{\mu_1} = \sum_{n=-\infty}^{\infty} \sum_{j=1}^3 \left[S_{lmj1}^{(1)} \left(K_n(k_j r) \right) a_{nj} + S_{lmj1}^{(2)} \left(I_n(k_j r) \right) b_{nj} \right] e^{i(\xi\eta + n\theta)},$$

where $l = r, \theta, \eta, m = r, \theta, \eta$;

$$T_{r11}^{(1)} = k_{11} K'_n(k_{11} r), \quad T_{r21}^{(1)} = -\frac{n}{r} K_n(k_{21} r), \quad T_{r31}^{(1)} = -\xi k_{31} K'_n(k_{31} r),$$

$$T_{\theta11}^{(1)} = \frac{n}{r} K_n(k_{11} r), \quad T_{\theta21}^{(1)} = -k_{21} K'_n(k_{21} r)i, \quad T_{\theta31}^{(1)} = -\frac{n}{r} \xi K_n(k_{31} r)i,$$

$$T_{\eta11}^{(1)} = \xi K_n(k_{11} r)i, \quad T_{\eta21}^{(1)} = 0, \quad T_{\eta31}^{(1)} = -k_{31}^2 K_n(k_{31} r)i,$$

$$S_{rr11}^{(1)} = 2 \left(k_{11}^2 + \frac{n^2}{r^2} - \frac{\lambda_1 M_{p1}^2 \xi^2}{2\mu_1} \right) K_n(k_{11}r) - \frac{2k_{11}K'_n(k_{11}r)}{r}, \quad S_{rr21}^{(1)} = \frac{2n}{r^2} K_n(k_{21}r) - \frac{2k_{21}K'_n(k_{21}r)}{r}, \quad S_{rr31}^{(1)} = -2\xi \left(k_{31}^2 + \frac{n^2}{r^2} \right) K_n(k_{31}r) + \frac{2\xi k_{31}K'_n(k_{31}r)}{r},$$

$$S_{\theta\theta11}^{(1)} = -2 \left(\frac{n^2}{r^2} + \frac{\lambda_1 M_{p1}^2 \xi^2}{2\mu_1} \right) K_n(k_{11}r) + \frac{2k_{11}K'_n(k_{11}r)}{r}, \quad S_{\theta\theta21}^{(1)} = -\frac{2nK_n(k_{21}r)}{r^2} + \frac{2nk_{21}K'_n(k_{21}r)}{r}, \quad S_{\theta\theta31}^{(1)} = \frac{2\xi n^2 K_n(k_{31}r)}{r^2} - \frac{2\xi k_{31}K'_n(k_{31}r)}{r},$$

$$S_{\eta\eta11}^{(1)} = -2\xi^2 \left(\frac{1 + \lambda_1 M_{p1}^2}{2\mu_1} \right) K_n(k_{11}r), \quad S_{\eta\eta21}^{(1)} = 0, \quad S_{\eta\eta31}^{(1)} = 2m_{31}^2 \xi^3 K_n(k_{31}r),$$

$$S_{r\theta11}^{(1)} = \left(-\frac{2nK_n(k_{11}r)}{r^2} + \frac{2nk_{11}K'_n(k_{11}r)}{r} \right) i, \quad S_{r\theta21}^{(1)} = \left(-\left(k_{21}^2 + \frac{2n^2}{r^2} \right) K_n(k_{21}r) + \frac{2k_{21}K'_n(k_{21}r)}{r} \right) i,$$

$$S_{r\theta31}^{(1)} = \left(\frac{2n\xi K_n(k_{31}r)}{r^2} - \frac{2n\xi k_{31}K'_n(k_{31}r)}{r} \right) i,$$

$$S_{\theta\eta11}^{(1)} = -\frac{2n\xi K_n(k_{11}r)}{r}, \quad S_{\theta\eta21}^{(1)} = \xi k_{21}K'_n(k_{21}r), \quad S_{\theta\eta31}^{(1)} = \frac{n\xi^2 (1 + m_{31}^2) K_n(k_{31}r)}{r},$$

$$S_{r\eta11}^{(1)} = 2\xi k_{11}K'_n(k_{11}r)i, \quad S_{r\eta21}^{(1)} = -\frac{\xi nK_n(k_{21}r)i}{r}, \quad S_{r\eta31}^{(1)} = -\xi^2 k_{31} (1 + m_{31}^2) K'_n(k_{31}r)i,$$

$K'_n(k_{j1}r) = \frac{dK_n(k_{j1}r)}{d(k_{j1}r)}$; $T_{lj1}^{(2)}$, $S_{lmj1}^{(2)}$ are derived from $T_{lj1}^{(1)}$, $S_{lmj1}^{(1)}$ replacing K_n with I_n ;

$$u_{l2}^* = \sum_{n=-\infty}^{\infty} \sum_{j=1}^3 \left[T_{lj2}^{(1)} (K_n(k_{j2}r)) a_{nj+3} + T_{lj2}^{(2)} (I_n(k_{j2}r)) a_{nj+6} \right] e^{i(\xi\eta+n\theta)},$$

$$\frac{\sigma_{lm2}^*}{\mu_2} = \sum_{n=-\infty}^{\infty} \sum_{j=1}^3 \left[S_{lmj2}^{(1)} (K_n(k_{j2}r)) a_{nj+3} + S_{lmj2}^{(2)} (I_n(k_{j2}r)) a_{nj+6} \right] e^{i(\xi\eta+n\theta)},$$

where $l = r, \theta, \eta, m = r, \theta, \eta$;

$$T_{r12}^{(1)} = k_{12}K'_n(k_{12}r), \quad T_{r22}^{(1)} = -\frac{n}{r} K_n(k_{22}r), \quad T_{r32}^{(1)} = -\xi k_{32}K'_n(k_{32}r),$$

$$T_{\theta12}^{(1)} = \frac{n}{r} K_n(k_{12}r)i, \quad T_{\theta22}^{(1)} = -k_{22}K'_n(k_{22}r)i, \quad T_{\theta32}^{(1)} = -\frac{n}{r} \xi K_n(k_{32}r)i,$$

$$T_{\eta12}^{(1)} = \xi K_n(k_{12}r)i, \quad T_{\eta22}^{(1)} = 0, \quad T_{\eta32}^{(1)} = -k_{32}^2 K_n(k_{32}r)i,$$

$$S_{rr12}^{(1)} = 2 \left(k_{12}^2 + \frac{n^2}{r^2} - \frac{\lambda_2 M_{p2}^2 \xi^2}{2\mu_2} \right) K_n(k_{12}r) - \frac{2k_{12}K'_n(k_{12}r)}{r}, \quad S_{rr22}^{(1)} = \frac{2n}{r^2} K_n(k_{22}r) - \frac{2k_{22}K'_n(k_{22}r)}{r},$$

$$S_{rr32}^{(1)} = -2\xi \left(k_{32}^2 + \frac{n^2}{r^2} \right) K_n(k_{32}r) + \frac{2\xi k_{32}K'_n(k_{32}r)}{r},$$

$$S_{\theta\theta12}^{(1)} = -2 \left(\frac{n^2}{r^2} + \frac{\lambda_2 M_{p2}^2 \xi^2}{2\mu_2} \right) K_n(k_{12}r) + \frac{2k_{12}K'_n(k_{12}r)}{r}, \quad S_{\theta\theta22}^{(1)} = -\frac{2nK_n(k_{22}r)}{r^2} + \frac{2nk_{22}K'_n(k_{22}r)}{r}, \quad S_{\theta\theta32}^{(1)} = \frac{2\xi n^2 K_n(k_{32}r)}{r^2} - \frac{2\xi k_{32}K'_n(k_{32}r)}{r},$$

$$S_{\eta\eta12}^{(1)} = -2\xi^2 \left(\frac{1 + \lambda_2 M_{p2}^2}{2\mu_2} \right) K_n(k_{12}r), \quad S_{\eta\eta22}^{(1)} = 0, \quad S_{\eta\eta32}^{(1)} = 2m_{32}^2 \xi^3 K_n(k_{32}r),$$

$$S_{r\theta12}^{(1)} = \left(-\frac{2nK_n(k_{12}r)}{r^2} + \frac{2nk_{12}K'_n(k_{12}r)}{r} \right) i, \quad S_{r\theta22}^{(1)} = \left(-\left(k_{22}^2 + \frac{2n^2}{r^2} \right) K_n(k_{22}r) + \frac{2k_{22}K'_n(k_{22}r)}{r} \right) i,$$

$$S_{r\theta32}^{(1)} = \left(\frac{2n\xi K_n(k_{32}r)}{r^2} - \frac{2n\xi k_{32}K'_n(k_{32}r)}{r} \right) i,$$

$$S_{\theta\eta12}^{(1)} = -\frac{2n\xi K_n(k_{12}r)}{r}, \quad S_{\theta\eta22}^{(1)} = \xi k_{22}K'_n(k_{22}r), \quad S_{\theta\eta32}^{(1)} = \frac{n\xi^2 (1 + m_{32}^2) K_n(k_{32}r)}{r},$$

$$S_{r\eta12}^{(1)} = 2\xi k_{12}K'_n(k_{12}r)i, \quad S_{r\eta22}^{(1)} = -\frac{\xi n K_n(k_{22}r)i}{r}, \quad S_{r\eta32}^{(1)} = -\xi^2 k_{32} (1 + m_{32}^2) K'_n(k_{32}r)i,$$

$K'_n(k_{j2}r) = \frac{dK_n(k_{j2}r)}{d(k_{j2}r)}$; $T_{lj2}^{(2)}$, $S_{lmj2}^{(2)}$ are derived from $T_{lj2}^{(1)}$, $S_{lmj2}^{(1)}$ replacing K_n with I_n .

In the steady state, the dependence of all the values on η has the form (5), hence

$$u_{0j}(\theta, \eta) = \sum_{n=-\infty}^{\infty} u_{0nj} e^{jn\theta} e^{i\xi\eta}, \quad j = r, \theta, \eta.$$

By substituting the last expressions in (2), we obtain

$$\varepsilon_1^2 u_{0n\eta} + \nu_{02} n \xi_0 u_{0n\theta} - 2i\nu_0 \xi_0 u_{0nr} = G_0(P_{n\eta} - q_{n\eta}),$$

$$\nu_{02} n \xi_0 u_{0n\eta} + \varepsilon_2^2 u_{0n\theta} - 2iu_{0nr} = G_0(P_{n\theta} - q_{n\theta}),$$

$$2i\nu_0 \xi_0 u_{0n\eta} + 2iu_{0n\theta} + \varepsilon_3^2 u_{0nr} = G_0(P_{nr} - q_{nr}),$$

where $\varepsilon_1^2 = \alpha_0^2 - \varepsilon_0^2$, $\varepsilon_2^2 = \beta_0^2 - \varepsilon_0^2$, $\varepsilon_3^2 = \gamma_0^2 - \varepsilon_0^2$, $\xi_0 = \xi R$,

$$\alpha_0^2 = 2\xi_0^2 + \nu_{01} n^2, \quad \beta_0^2 = \nu_{01} \xi_0^2 + 2n^2, \quad \gamma_0^2 = \chi^2 (\xi_0^2 + n^2)^2 + 2, \quad \varepsilon_0^2 = \nu_{01} \xi_0^2 M_{s0}^2,$$

$$\nu_{01} = 1 - \nu_0, \quad \nu_{02} = 1 + \nu_0, \quad M_{s0} = c / c_{s0}, \quad c_{s0} = (\mu_0 / \rho_0)^{1/2}, \quad \chi^2 = \frac{h_0^2}{6R^2}, \quad G_0 = -\left(\nu_{01} R^2 \right) / (\mu_0 h_0);$$

when $r = R$: $q_{nj} = (\sigma_{rj2}^*)_n$, $j = \eta, \theta, r$.

From these equations we find

$$u_{0n\eta} = \frac{G_0}{\delta_n} \sum_{j=1}^3 \delta_{\eta j} (P_{nj} - q_{nj}), \quad u_{0n\theta} = \frac{G_0}{\delta_n} \sum_{j=1}^3 \delta_{\theta j} (P_{nj} - q_{nj}), \quad u_{0nr} = \frac{G_0}{\delta_n} \sum_{j=1}^3 \delta_{rj} (P_{nj} - q_{nj}).$$

Here $\delta_n = \delta_{|\eta|} = (\varepsilon_1 \varepsilon_2 \varepsilon_3)^2 - (\varepsilon_1 \xi_1)^2 - (\varepsilon_2 \xi_2)^2 - (\varepsilon_3 \xi_3)^2 + 2 \xi_1 \xi_2 \xi_3$,

$$\delta_{\eta 1} = (\varepsilon_2 \varepsilon_3)^2 - \xi_1^2, \quad \delta_{\eta 2} = \xi_1 \xi_2 - \xi_3 \xi_3^2, \quad \delta_{\eta 3} = i(\varepsilon_2^2 \xi_2 - \xi_1 \xi_3),$$

$$\delta_{\theta 1} = \delta_{\eta 2}, \quad \delta_{\theta 2} = (\varepsilon_1 \varepsilon_3)^2 - \xi_2^2, \quad \delta_{\theta 3} = i(\varepsilon_1^2 \xi_1 - \xi_2 \xi_3),$$

$$\delta_{r1} = -\delta_{\eta 3}, \quad \delta_{r2} = -\delta_{\theta 3}, \quad \delta_{r3} = (\varepsilon_1 \varepsilon_2)^2 - \xi_3^2, \quad \xi_1 = 2n, \quad \xi_2 = 2\nu_0 \xi_0, \quad \xi_3 = \nu_0 \xi_0 n;$$

for P_{nj} , and q_{nj} the index $j = 1$ corresponds to the index η , $j = 2 - \theta$, $j = 3 - r$.

The unknown coefficients a_{n1}, \dots, a_{n9} are obtained from the following boundary conditions:

$$\text{when } r = R_1 \quad u_{j1}^* = u_{j2}^*, \quad \sigma_{rj1}^* = \sigma_{rj2}^*,$$

$$\text{when } r = R_2 \quad u_{j2}^* = u_{0j}, \quad j = r, \theta, \eta.$$

By substituting the corresponding expressions into the boundary conditions and by equating the coefficients of the Fourier-Bessel series with $e^{in\theta}$, for each value of $n = 0, \pm 1, \pm 2, \dots$ we obtain a system of linear algebraic equations which has a single solution if its determinant $\Delta_n(\xi, c) \neq 0$. From these systems of equations we determine the coefficients a_{n1}, \dots, a_{n9} .

The response of the shell and the half-space to an aperiodic load of the form $P(\theta, \eta) = p(\theta)p(\eta)$ moving with constant velocity can be found by superposition, using the representation of the load and SSS components of the enclosing layer of the shell and the half-space in the form of Fourier integrals

$$\begin{aligned} P(\theta, \eta) &= \frac{1}{2\pi} \int_{-\infty}^{\infty} P^*(\theta, \xi) e^{i\xi\eta} d\xi = p(\theta)p(\eta) = p(\theta) \frac{1}{2\pi} \int_{-\infty}^{\infty} p^*(\xi) e^{i\xi\eta} d\xi, \\ P_m(\theta, \eta) &= \frac{1}{2\pi} \int_{-\infty}^{\infty} P_m^*(\theta, \xi) e^{i\xi\eta} d\xi = p_m(\theta)p(\eta) = p_m(\theta) \frac{1}{2\pi} \int_{-\infty}^{\infty} p^*(\xi) e^{i\xi\eta} d\xi; \\ u_{lk}(r, \theta, \eta) &= \frac{1}{2\pi} \int_{-\infty}^{\infty} u_{lk}^*(r, \theta, \xi) p^*(\xi) d\xi, \\ \sigma_{lmk}(r, \theta, \eta) &= \frac{1}{2\pi} \int_{-\infty}^{\infty} \sigma_{lmk}^*(r, \theta, \xi) p^*(\xi) d\xi. \end{aligned} \tag{11}$$

$$\text{Here } l = r, \theta, \eta, m = r, \theta, \eta, k = 1, 2; \quad p^*(\xi) = \int_{-\infty}^{\infty} p(\eta) e^{-i\xi\eta} d\eta.$$

Any numerical integration method can be used to calculate displacements and stresses (11) if the determinants $\Delta_n(\xi, c) \neq 0$ ($n = 0, \pm 1, \pm 2, \dots$). These conditions are fulfilled when the load velocity c is less than its critical velocities $c_{(n)*}$, whose values depend on the number n and can be less than the Rayleigh wave velocity in the half-space. Calculations show that the minimum critical velocity occurs when $n = 0$, i.e. $\min c_{(n)*} = c_{(0)*}$ (Ukrainets, 2006; Alexeyeva, 2009).

In the case of a shell without an enclosing layer ($R_1 = R_2 = R$) the solution of the problem is simplified. To obtain the solution in this case, all relations for the enclosing layer ($k = 2$) of a two-layer shell should be excluded in the solution given here. In equations (2) the reactions $q_j = \sigma_{rj2}$ are replaced by $q_j = \sigma_{rj1}$. The coefficients a_{n1}, a_{n2}, a_{n3} are determined from the boundary conditions: when $r = R$ $u_{j1}^* = u_{0j}$, $j = r, \theta, \eta$ (Ukrainets, 2006).

3.2 Numerical experiments

Based on the obtained solution to the problem, the authors developed computer programs for calculating critical load speeds, as well as the SSS components of the shell and its surrounding elastic half-space. When carrying out numerical experiments using these programs for the single-layer shell considered in Alexeyeva (2020) (where the analytical solution of a similar problem was based on the exact equations of the theory of elasticity), which in this case was represented in the form of a two-layer shell with rigidly conjugated layers considered here, numerical results coinciding with Alexeyeva (2020) were obtained.

The solution obtained will be used to study the influence of the enclosing layer of the shallow underground pipeline on its dynamic behavior under the action of an axisymmetric normal load moving at a velocity of $c = 100$ m/s. The load exerts uniform pressure on the inner surface of the pipeline ($r = R_2 = R = 1$ m) within the interval $|\eta| \leq l_0 = 0.2R$ (Fig. 2). This is a similar type of load to that accepted in the calculation of main gas pipelines (Gershtejn et al., 1973).

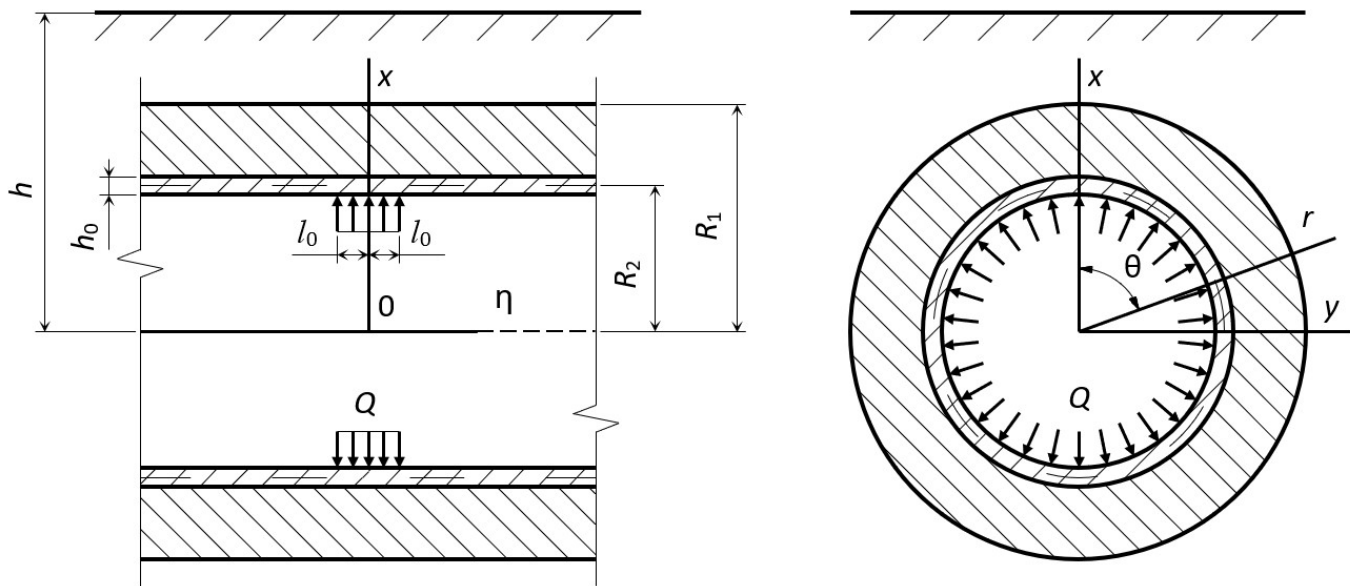


Figure 2 The action of a load with intensity Q on the pipeline

The depth of the pipeline in the rock body ($v_1 = 0.25$, $\mu_1 = \mu = 4.0 \cdot 10^9$ Pa, $\rho_1 = 2.6 \cdot 10^3$ kg/m³; $c_{s1} = 1240.35$ m/c, $c_R = 1140.42$ m/c) $h = 2R$. A pipeline may be considered as a thin-walled steel shell ($R_2 = R = 1$ m, $h_0/R = 0.02$; $v_0 = 0.3$, $\mu_0 = 8.08 \cdot 10^{10}$ Pa, $\rho_0 = 7.8 \cdot 10^3$ kg/m³) without an enclosing layer and with an enclosing layer of thickness $h_c = R_1 - R_2$. As an enclosing layer, we consider a shell constructed from a material with a stiffness less than that of the rock body material ($v_2 = 0.25$, $\mu_2 = 2.8 \cdot 10^9$ Pa, $\rho_2 = 2.65 \cdot 10^3$ kg/m³; $c_{s2} = 1028$ m/c) or a shell constructed from a material with a stiffness greater than that of the rock body material ($v_2 = 0.2$, $\mu_2 = 1.21 \cdot 10^{10}$ Pa, $\rho_2 = 2.5 \cdot 10^3$ kg/m³; $c_{s2} = 2200$ m/c). The calculations have demonstrated that for all pipelines under consideration $c < c_{(0)}*$.

The intensity Q (Pa) of the transport load acting on the pipeline is chosen so that the total load along the entire length of the loading section $2l_0$ is equal to the concentrated normal ring load with intensity P° (N/m), i.e. $Q = P^\circ / 2l_0$. Let us introduce the following designations (we will omit the indices $k = 1, 2$ in the designations of displacements and stresses):

$$\dot{u}_r = u_r \mu / P^\circ \text{ (m)}, \dot{\sigma}_{rr} = \sigma_{rr} / P^\circ, \dot{\sigma}_{\theta\theta} = \sigma_{\theta\theta} / P^\circ, \dot{\sigma}_{\eta\eta} = \sigma_{\eta\eta} / P^\circ, \dot{u}_x = u_x \mu / P^\circ \text{ (m)}, \dot{u}_y = u_y \mu / P^\circ \text{ (m)}, \dot{\sigma}_{yy} = \sigma_{yy} / P^\circ, \text{ where } P^\circ = P^\circ / m \text{ (Pa).}$$

Note: on the graphs \dot{u}_r (m) and \dot{u}_x (m) presented in this section, a different scale was taken for their values than for the transverse dimensions of the pipeline.

The results of the SSS calculations of the rock body surface or enclosing layer ($r = R = 1$ m) of different thickness h_c in the xy -Cartesian plane ($\eta = 0$) in contact with the steel shell are presented in Table 1. Fig. 3 shows the diagrams of radial displacements on the contour of these surfaces.

Table 1 The SSS components of the rock body surface or enclosing layer ($r = R = 1$ m) in the xy -Cartesian plane ($\eta = 0$) in contact with the steel shell

h_c/R	Comp. SSS	$ \theta $, degrees									
		0	20	40	60	80	100	120	140	160	180
Pipeline without an enclosing layer											
0	u_r^*	0.45	0.44	0.41	0.38	0.36	0.35	0.35	0.35	0.36	0.36
	σ_{rr}^*	-2.04	-2.04	-2.03	-2.03	-2.03	-2.04	-2.04	-2.05	-2.05	-2.06
	$\sigma_{\theta\theta}^*$	0.18	0.19	0.23	0.24	0.23	0.21	0.19	0.17	0.15	0.14
	$\sigma_{\eta\eta}^*$	-0.96	-0.95	-0.94	-0.92	-0.92	-0.92	-0.92	-0.92	-0.93	-0.93
Pipeline with an enclosing layer when $\mu_2 < \mu_1$											
0,1	u_r^*	0.49	0.47	0.44	0.41	0.39	0.38	0.38	0.38	0.39	0,39
	σ_{rr}^*	-2.02	-2.02	-2.01	-2.01	-2.01	-2.02	-2.02	-2.03	-2.03	-2.04
	$\sigma_{\theta\theta}^*$	-0.01	0.0	0.02	0.03	0.03	0.01	0.0	-0.02	-0.03	-0.04
	$\sigma_{\eta\eta}^*$	-0.85	-0.84	-0.83	-0.83	-0.82	-0.82	-0.83	-0.83	-0.83	-0.83
0,5	u_r^*	0.56	0.55	0.51	0.47	0.44	0.43	0.43	0.44	0.45	0.45
	σ_{rr}^*	-1.96	-1.95	-1.95	-1.94	-1.95	-1.95	-1.96	-1.97	-1.97	-1.98
	$\sigma_{\theta\theta}^*$	0.11	0.12	0.15	0.16	0.16	0.14	0.12	0.10	0.08	0.08
	$\sigma_{\eta\eta}^*$	-0.84	-0.84	-0.83	-0.82	-0.82	-0.82	-0.82	-0.82	-0.83	-0.83
Pipeline with an enclosing layer when $\mu_2 > \mu_1$											
0,1	u_r^*	0.34	0.33	0.31	0.29	0.28	0.27	0.27	0.28	0.28	0.28
	σ_{rr}^*	-2.11	-2.10	-2.09	-2.07	-2.07	-2.07	-2.09	-2.10	-2.11	-2.12
	$\sigma_{\theta\theta}^*$	1.46	1.47	1.47	1.43	1.38	1.35	1.35	1.37	1.38	1.39
	$\sigma_{\eta\eta}^*$	-1.55	-1.54	-1.53	-1.52	-1.51	-1.50	-1.49	-1.49	-1.48	-1.48
0,5	u_r^*	0.22	0.21	0.20	0.18	0.18	0.17	0.17	0.17	0.17	0.17
	σ_{rr}^*	-2.21	-2.21	-2.20	-2.19	-2.19	-2.19	-2.20	-2.21	-2.21	-2.22
	$\sigma_{\theta\theta}^*$	0.62	0.63	0.66	0.66	0.65	0.62	0.60	0.59	0.58	0.59
	$\sigma_{\eta\eta}^*$	-1.33	-1.32	-1.30	-1.29	-1.28	-1.27	-1.27	-1.27	-1.27	-1.27

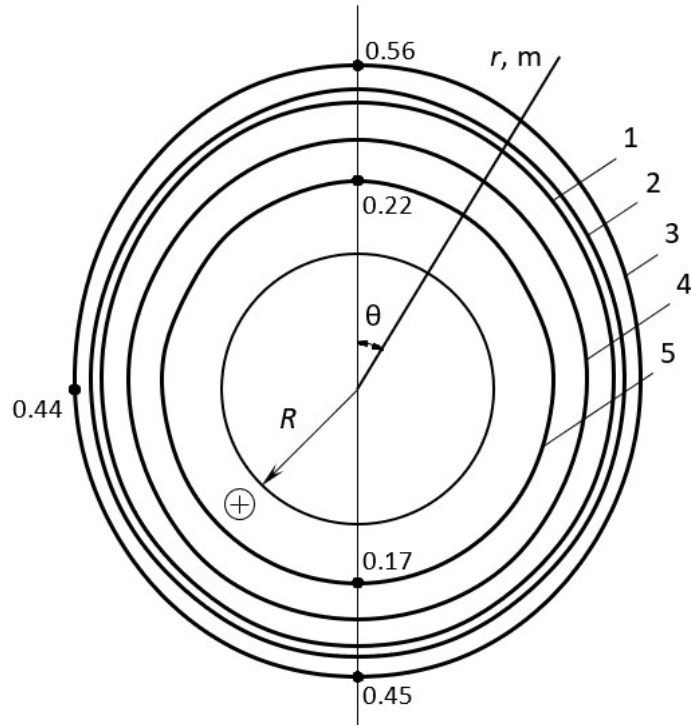
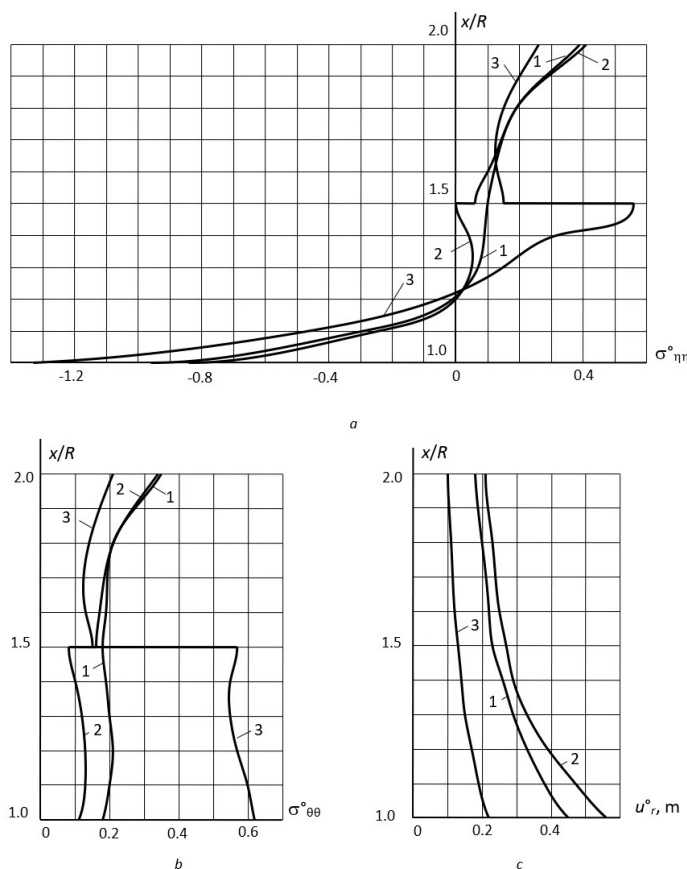
**Figure 3** Radial displacement diagrams u_r^* , m on the contour of the surfaces in contact with the steel shell ($r = R = 1$ m, $\eta = 0$). Curve designations: 1 – a pipeline without an enclosing layer; 2, 3 – a pipeline with an enclosing layer when $\mu_2 < \mu_1$ ($2 - h_c/R = 0.1$; $3 - h_c/R = 0.5$); 4, 5 – a pipeline with an enclosing layer when $\mu_2 > \mu_1$ ($4 - h_c/R = 0.1$; $5 - h_c/R = 0.5$).

Table 2 shows the results of the calculation of the SSS of the enclosing layer and the rock body at the points of the x -axis directed to the ground surface. Fig. 4 shows the curves of changes of normal stresses and radial displacements with distance from the steel shell towards the ground surface ($\eta = y = 0$).

Table 2 The SSS components of the enclosing layer and the rock body at the points of the x -axis

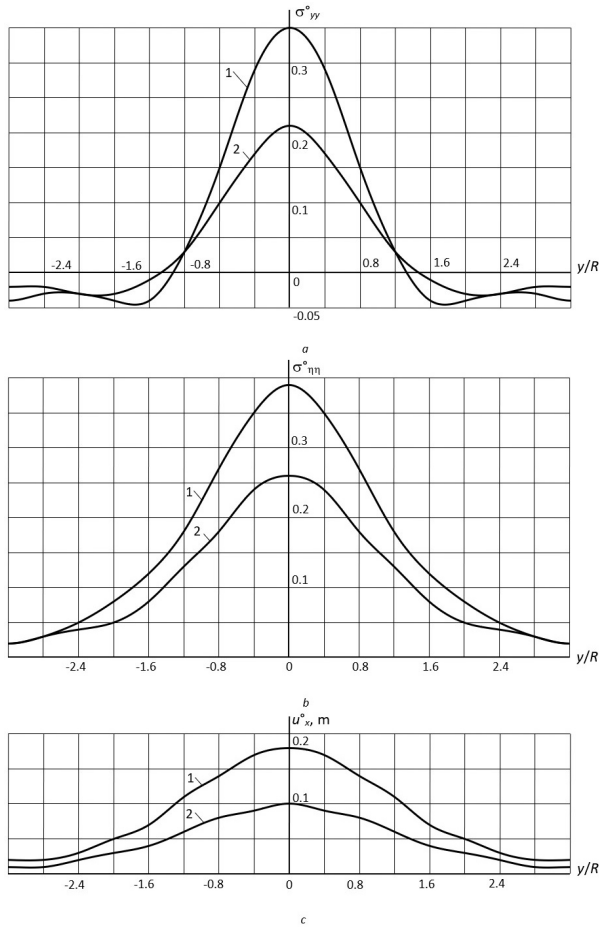
Comp. SSS	x/R								
	1.0	1.1	1.2	1.3	1.4	1.5	1.6	1.8	2.0
Pipeline without an enclosing layer									
u^*_r	0.45	0.38	0.33	0.29	0.26	0.23	0.22	0.20	0.18
σ^*_{rr}	-2.04	-1.65	-1.20	-0.83	-0.57	-0.38	-0.25	-0.07	0.0
$\sigma^*_{\theta\theta}$	0.18	0.20	0.21	0.20	0.19	0.18	0.19	0.21	0.35
$\sigma^*_{\eta\eta}$	-0.96	-0.29	-0.01	0.07	0.09	0.10	0.12	0.19	0.39
Pipeline with an enclosing layer when $\mu_2 < \mu_1$ ($h_c/R = 0.5$)									
u^*_r	0.56	0.47	0.39	0.33	0.29	0.27	0.25	0.23	0.21
σ^*_{rr}	-1.96	-1.58	-1.16	-0.82	-0.58	-0.39	-0.25	-0.06	0.0
$\sigma^*_{\theta\theta}$	0.11	0.13	0.13	0.12	0.10	0.08	0.17	0.21	0.34
$\sigma^*_{\eta\eta}$	-0.84	-0.24	0.0	0.05	0.04	0.0	0.10	0.19	0.41
Pipeline with an enclosing layer when $\mu_2 > \mu_1$ ($h_c/R = 0.5$)									
u^*_r	0.22	0.19	0.17	0.15	0.14	0.13	0.12	0.11	0.10
σ^*_{rr}	-2.21	-1.75	-1.22	-0.78	-0.46	-0.25	-0.15	-0.03	0.0
$\sigma^*_{\theta\theta}$	0.62	0.60	0.57	0.55	0.55	0.57	0.13	0.14	0.21
$\sigma^*_{\eta\eta}$	-1.33	-0.46	-0.05	0.15	0.32	0.56	0.13	0.15	0.26

**Figure 4** Changes in stresses $\sigma^*_{\eta\eta}$ (a), $\sigma^*_{\theta\theta}$ (b) and displacements u^*_r (c) with distance from the steel shell ($\eta = y = 0$). Curve designations: 1 – a pipeline without an enclosing layer; 2 – a pipeline with an enclosing layer when $\mu_2 < \mu_1$ ($h_c/R = 0.5$); 3 – a pipeline with an enclosing layer when $\mu_2 > \mu_1$ ($h_c/R = 0.5$).

The results of the SSS calculations of the ground surface ($x = h$) in the xy -Cartesian plane ($\eta = 0$) are presented in Table 3. Fig. 5 in this plane shows the curves of change of the SSS components of the ground surface.

Table 3 The SSS components of the ground surface in the xy-Cartesian plane

h_c/R	Comp. SSS	y/R								
		0.0	0.4	0.8	1.2	1.6	2.0	2.4	2.8	3.2
Pipeline without an enclosing layer										
0	u_x^*	0.18	0.17	0.14	0.11	0.07	0.05	0.03	0.02	0.02
	u_y^*	0.0	0.04	0.06	0.07	0.06	0.05	0.04	0.04	0.03
	σ_{yy}^*	0.35	0.29	0.15	0.03	-0.04	-0.04	-0.03	-0.03	-0.04
	$\sigma_{\eta\eta}^*$	0.39	0.35	0.27	0.18	0.12	0.08	0.05	0.03	0.02
Pipeline with an enclosing layer when $\mu_2 < \mu_1$										
0,1	u_x^*	0.19	0.18	0.14	0.11	0.07	0.05	0.03	0.02	0.02
	u_y^*	0.0	0.04	0.06	0.07	0.06	0.05	0.04	0.04	0.03
	σ_{yy}^*	0.35	0.28	0.16	0.04	-0.02	-0.03	-0.04	-0.05	-0.04
	$\sigma_{\eta\eta}^*$	0.39	0.36	0.27	0.19	0.12	0.08	0.05	0.03	0.02
0,5	u_x^*	0.21	0.20	0.16	0.11	0.07	0.05	0.03	0.02	0.02
	u_y^*	0.0	0.04	0.06	0.07	0.07	0.06	0.05	0.04	0.03
	σ_{yy}^*	0.34	0.30	0.18	0.05	-0.02	-0.03	-0.04	-0.05	-0.06
	$\sigma_{\eta\eta}^*$	0.41	0.37	0.29	0.20	0.13	0.08	0.05	0.04	0.03
Pipeline with an enclosing layer when $\mu_2 > \mu_1$										
0,1	u_x^*	0.14	0.13	0.10	0.08	0.05	0.04	0.02	0.02	0.01
	u_y^*	0.0	0.03	0.05	0.05	0.05	0.04	0.03	0.02	0.02
	σ_{yy}^*	0.28	0.23	0.13	0.03	-0.02	-0.03	-0.03	-0.03	-0.03
	$\sigma_{\eta\eta}^*$	0.34	0.30	0.23	0.16	0.10	0.07	0.05	0.03	0.02
0,5	u_x^*	0.10	0.09	0.08	0.06	0.04	0.03	0.02	0.01	0.01
	u_y^*	0.0	0.02	0.03	0.04	0.04	0.03	0.02	0.02	0.01
	σ_{yy}^*	0.21	0.17	0.10	0.03	-0.01	-0.03	-0.03	-0.02	-0.02
	$\sigma_{\eta\eta}^*$	0.26	0.24	0.18	0.13	0.08	0.05	0.04	0.03	0.02

**Figure 5** Changes in the SSS components of the ground surface in the xy-Cartesian plane. Curve designations: 1 – a pipeline without an enclosing layer; 2 – a pipeline with an enclosing layer when $\mu_2 > \mu_1$ and $h_c/R = 0.5$.

4 DISCUSSION

From the analysis of the calculation results (Table 1) it follows that the stresses $\sigma_{\theta\theta}$ of the surface of the rock mass or enclosing layer of the pipeline in contact with the steel shell ($r = R = 1$ m) in the coordinate plane xy ($\eta = 0$) are tensile, and stresses σ_{rr} , $\sigma_{\eta\eta}$ are compressive (with the exception of stresses $\sigma_{\theta\theta}$ at $\mu_2 < \mu_1$ and $h_c/R = 0.1$, which, depending on Θ , have different signs). If the steel shell is enclosed by a layer of material less rigid than the material of the rock body ($\mu_2 < \mu_1$), the displacements u_r of contact points increase and the values of normal stresses $|\sigma_{rr}|$, $|\sigma_{\eta\eta}|$ and $\sigma_{\theta\theta}$ in these points decrease (Table 1, Fig. 3). Moreover, this trend for u_r and $|\sigma_{rr}|$ increases with increasing layer thickness. When the steel shell is enclosed by a layer more rigid than the material of the rock body ($\mu_2 > \mu_1$), the opposite effect occurs.

As it can be seen from the calculations carried out for the pipeline under consideration (both without and with an enclosing layer of material of different stiffness), with vertical distance from the pipeline ($x \rightarrow -\infty$, $\eta = 0$) all components of the SSS of the rock body attenuate to almost zero values when $|x| = 4\div 5R$. As it moves away from the pipeline toward the ground surface until it reaches the ground surface, the dynamic impact of the load on the rock body remains significant, as shown in Table 2 and Figure 4. If $\mu_2 > \mu_1$, then the impact is less than in the other cases. At $x/R = 2$ (on the earth's surface) $\sigma_{rr} = \sigma_{xx} = 0$. As calculations have shown, at the same point $\sigma_{r\theta} = \sigma_{xy} = 0$ and $\sigma_{\eta\eta} = \sigma_{x\eta} = 0$, which indicates the exact fulfillment of the boundary conditions on the earth's surface. For a pipeline with an enclosing layer at $h_c/R = 0.5$, as it can be seen from the graphs presented in Fig. 4, changes in normal stresses $\sigma_{\theta\theta}$, $\sigma_{\eta\eta}$ along the x -axis are more complex than changes in radial displacements u_r . When crossing the interface between the enclosing layer and the rock body, "jumps" are observed in the graphs, that is, there is a sharp change in the values of these stresses: their increase, at $\mu_2 < \mu_1$ and their decrease, with $\mu_2 > \mu_1$.

From the analysis of the results of the calculations of the SSS of the ground surface (Table 3, Fig. 5), it can be seen that the material of the pipeline enclosing layer ($\mu_2 > \mu_1$), which is stiffer than the material of the rock body, reduces the dynamic effect of the transport load on it, compared to the effect of this load on the pipeline without such an enclosing layer. The encapsulating layer, which is less rigid than the rock body ($\mu_2 < \mu_1$), has a negligible effect on the ground surface. The displacement u_x and stress $\sigma_{\theta\theta}$, $\sigma_{\eta\eta}$ of the earth's surface have the greatest values at $y = 0$ and quickly decrease as $|y|$ increases. When $y = 0$, displacement $u_y = 0$. As y increases, the value of u_y first increases and then decreases. It should be noted that, as calculations have shown, the components σ_{xx} , σ_{xy} , $\sigma_{x\eta}$ of the SSS of the earth's surface are equal to zero, that is, the boundary conditions on it are strictly satisfied.

5 CONCLUSION

A model problem is solved to study the dynamics of a shallow underground two-layer pipeline under the influence of transport loads. The pipeline is modeled as an extended circular cylindrical two-layer shell with a thin inner (bearing) layer and a thick outer (enclosing) layer (in a special case, a pipeline without an enclosing layer is considered). Unlike similar works, where the rock body surrounding the pipeline is represented as an elastic space, this paper provides it as an elastic half-space. In this case, the solution to the problem becomes much more complicated due to the perceptible deformation of the ground surface and its influence on the stress concentration in the vicinity of the pipeline during the diffraction of reflected waves.

The numerical experiments considered the case of a moving axisymmetric normal load exerting uniform stress on the pipeline (without an enclosing layer and with an enclosing layer of different thickness and material stiffness), which exerts uniform pressure on its inner surface in a certain interval. With the help of the computer program developed by the authors, the results of the SSS calculations of the enclosing layer of the pipeline and the surrounding rock body in the plane normal to the pipeline axis, passing through the middle of the moving load, were obtained and analyzed. It was demonstrated that if the material of the enclosing layer of the pipeline is more rigid than that of the rock body, the dynamic effect of the moving load on the rock body is reduced.

The developed calculation method is recommended for the dynamic calculation of shallow underground pipelines under the influence of transport loads. It allows us to consider not only the physical and mechanical properties of rock materials and pipelines and their design features but also the depth of the pipeline, the type of transport load, and its velocity. By selecting materials and thicknesses of pipeline layers, it is possible, without reducing the accepted speed for an object moving along it, not only to ensure the safe operation of the pipeline, but also to reduce vibration of the earth's surface, which negatively affects the seismic resistance of nearby buildings and structures.

Author's Contributions: Conceptualization, S. Girnis and V. Ukrainets; Methodology, V. Ukrainets; Investigation, S. Girnis, V. Stanevich and L. Gorshkova; Software, V. Ukrainets and S. Girnis; Data curation, V. Stanevich; Writing - original draft, V. Ukrainets, V. Stanevich and L. Gorshkova; Writing - review & editing, S. Girnis.

Editor: Rogério José Marczak

References

- Alexeyeva, L. A. (2009). Dynamics of an elastic half-space with a reinforced cylindrical cavity under moving loads, International Applied Mechanics 45(9): 981–990. <https://doi.org/10.1007/s10778-010-0238-z>.
- Alexeyeva, L. A. (2020). Model of the dynamics of a tunnel and a shallow underground pipeline under the action of traffic loads (In Russian), Bulletin of the L. N. Gumilyov Eurasian National University. Mathematics. Computer Science. Mechanics Series 133(4): 28–39. <https://doi.org/10.32523/2616-7182/2020-133-4-28-39>.
- Boström, A., Yuan, Z. (2019). Benchmark solutions for vibrations from a moving source in a tunnel in a half-space, In Ground Vibrations from High-Speed Railways, ICE Publishing: 261–281. <https://doi.org/10.1680/gvfhsl.63792.261>.
- Girnis, S., Bulyga, L., Stanevich, V. (2023). Action of Moving Load on a Two-Layer Shell in Elastic Medium, In Lecture Notes in Networks and Systems 574: 2301–2311. https://doi.org/10.1007/978-3-031-21432-5_251.
- Coşkun, İ., Dolmaseven, D. (2017). Dynamic Response of a Circular Tunnel in an Elastic Half Space, Journal of Engineering 2017: 1–12. <https://doi.org/10.1155/2017/6145375>.
- Gershtejn, M. S., Kamershtejn, A. T., Prokořev, V. I. (1973). Problems of the dynamics of main pipelines (In Russian), Calculation of spatial structures 15: 78–86.
- Hussein, M. F. M., Hunt, H. E. M., Rikse, L., Gupta, S., Degrande, G., Talbot, J. P., François, S., Schevenels, M. (2010). Using the PiP Model for Fast Calculation of Vibration from a Railway Tunnel in a Multi-layered Half-Space, Noise and Vibration Mitigation for Rail Transportation Systems 38(1): 136–142. https://doi.org/10.1007/978-3-540-74893-9_19.
- Hussein, M. F. M., François, S., Schevenels, M., Hunt, H. E. M., Talbot, J. P., Degrande, G. (2014). The fictitious force method for efficient calculation of vibration from a tunnel embedded in a multi-layered half-space, Journal of Sound and Vibration 333(25): 6996–7018. <https://doi.org/10.1016/j.jsv.2014.07.020>.
- Kulińska, E. (2014). Pipeline Transportation of Solid Materials, China-USA Business Review 13(8): 527–539. <https://doi.org/10.17265/1537-1514/2014.08.003>.
- Lvovsky, V. M., Onishchenko, V. I., Pozhuev, V. I. (1974). Steady-state vibrations of a cylindrical shell in an elastic medium under the action of a moving load (In Russian), In Issues of strength and ductility. Dnipropetrovsk State University 1974: 98–110.
- Makashev, K. T. (2023). Dynamic response of unsupported and supported cavities in an elastic half-space under moving normal and torsional loads, Bulletin of the Karaganda University. Physics Series 112(4): 65–75. <https://doi.org/10.31489/2023ph4/65-75>.
- Novackij, V. (1975). Theory of elasticity, Mir, Moscow.
- Otarbaev, Zh. O. (2016). Numerical research of dynamic behavior of metropolitan main line tunnel under the action of transport load (In Russian), Bulletin of the National Engineering Academy of the Republic of Kazakhstan: 4, 81–87.
- Otarbaev, Zh. O. (2018). Influence of rate of running periodic load in three-layer lining of a tunnel upon deflected mode of surround massif (In Russian), Bulletin of the National Engineering Academy of the Republic of Kazakhstan 3: 64–72.
- Pozhuev, V. I. (1977). Effect of stiffness of the damping layer on the reaction of a cylindrical shell to an axisymmetric moving load, Soviet Applied Mechanics 13(9): 878–883. <https://doi.org/10.1007/BF00884796>.
- Pozhuev, V. I. (1978). Response of a cylindrical shell with filler to the action of a non-axisymmetric moving load (In Russian), News of the USSR Academy of Sciences. Mechanics of Solids 5: 106–112.
- Pozhuev, V. I. (1980). Reaction of three-layer cylindrical shell to the action of a moving load, Soviet Applied Mechanics 16(1): 24–29. <https://doi.org/10.1007/BF00884609>.
- Ukrainets, V. N. (2006). Dynamics of shallow tunnels and pipelines under the influence of moving loads (In Russian), Publisher of Pavlodar State University, Kazakhstan.
- Ukrainets, V. N. (2010). The action of a moving load on a thick-walled shell in an elastic half-space (In Russian), Bulletin of Pavlodar State University. A Series of Physical and Mathematical 4: 81–86.
- Yang, Y. B., Hung, H. H. (2008). Soil Vibrations Caused by Underground Moving Trains, Journal of Geotechnical and Geoenvironmental Engineering 134(11): 1633–1644. [https://doi.org/10.1061/\(ASCE\)1090-0241\(2008\)134:11\(1633\)](https://doi.org/10.1061/(ASCE)1090-0241(2008)134:11(1633)).
- Yerzhanov, Zh. S., Ajtaliev, Sh. M. (1989). The dynamics of tunnels and underground pipelines (In Russian), Nauka, Alma-Ata.

Yuan, Z., Boström, A., Cai, Y., Cao, Z. (2017). Closed-Form Analytical Solution for Vibrations from a Tunnel Embedded in a Saturated Poroeelastic Half-Space, *Journal of Engineering Mechanics* 143(9). [https://doi.org/10.1061/\(ASCE\)EM.1943-7889.0001302](https://doi.org/10.1061/(ASCE)EM.1943-7889.0001302).

Zhangabay, N., Ibraimova, U., Suleimenov, U., Moldagaliyev, A., Buganova, S., Jumabayev, A., Kolesnikov, A., Tursunkululy, T., Zhiyenkulkyzy, D., Khalelova, A., Liseitsev, Y. (2023). Factors affecting extended avalanche destructions on long-distance gas pipelines: Review, *Case Studies in Construction Materials* 19: e02376. <https://doi.org/10.1016/j.cscm.2023.e02376>.

Zhou, S. (2019). *Dynamics of Rail Transit Tunnel Systems*, Elsevier. <https://doi.org/10.1016/C2018-0-00080-8>.

Zhukenova, G.A. (2023). The impact of normal and tangential loads on a shallow tunnel (In Kazakh), *Bulletin of the L.N. Gumilyov Eurasian National University. Mathematics. Computer Science. Mechanics Series* 144(3): 12–22. <https://doi.org/10.32523/2616-7182/bulmathenu.2023/3.2>.